PROCEEDINGS OF SCIENCE

ONLINE ICRC 2021
THE ASTROPARTICLE PHYSICS CONFERENCE
Berlin | Germany
37th International Cosmic Ray Conference
12–23 July 2021

Decelerated sub-relativistic material with energy Injection

B. Betancourt Kamenetskaia,[a,b,*] **N. Fraija,**[c] **M. Dainotti,**[d,e,f,g] **A. Gálvan-Gámez,**[c] **R. Barniol Duran**[h] **and S. Dichiara**[i,j]

[a] *TUM Physics Department, Technical University of Munich, James-Franck-Straße, 85748 Garching, Germany*
[b] *LMU Physics Department, Ludwig Maxmillians University, Theresienstr. 37, 80333 Munich, Germany*
[c] *Instituto de Astronomía, Universidad Nacional Autónoma de México, Ciudad de México, México*
[d] *Physics Department, Stanford University, 382 Via Pueblo Mall, Stanford, USA*
[e] *Space Science Institute, Boulder, CO, USA*
[f] *Obserwatorium Astronomiczne, Uniwersytet Jagielloński, ul. Orla 171, 31-501 Kraków, Poland*
[g] *Interdisciplinary Theoretical & Mathematical Science Program, RIKEN(iTHEMS), 2-1 Hirosawa, Wako, Saitama, 351-0198, Japan*
[h] *Department of Physics and Astronomy, California State University, Sacramento, 6000 J Street, Sacramento, CA 95819-6041, USA*
[i] *Department of Astronomy, University of Maryland, College Park, MD 20742-4111, USA*
[j] *Astrophysics Science Division, NASA Goddard Space Flight Center, 8800 Greenbelt Road, Greenbelt, MD 20771, USA*
E-mail: boris_betancourt@ciencias.unam.mx, nifraija@astro.unam.mx

We investigate the evolution of the afterglow produced by the deceleration of the non-relativistic material due to its surroundings. The ejecta mass is launched into the circumstellar medium with equivalent kinetic energy expressed as a power-law velocity distribution $E \propto (\Gamma\beta)^{-\alpha}$. The density profile of this medium follows a power law $n(r) \propto r^{-k}$ with k the stratification parameter, which accounts for the usual cases of a constant medium ($k = 0$) and a wind-like medium ($k = 2$). A long-lasting central engine, which injects energy into the ejected material as ($E \propto t^{1-q}$) was also assumed. With our model, we show the predicted light curves associated with this emission for different sets of initial conditions and notice the effect of the variation of these parameters on the frequencies, timescales and intensities. The results are discussed in the Kilonova scenario.

37th International Cosmic Ray Conference (ICRC 2021)
July 12th – 23rd, 2021
Online – Berlin, Germany

*Presenter

PoS(ICRC2021)660

1. Introduction

Long-duration gamma-ray bursts [lGRBs; $T_{90} \gtrsim 2$ s; 1] are linked to supernovae [SNe; 2, 3] caused by the core collapse (CC) of dying massive stars [4, 5]. Short-duration gamma-ray bursts, on the other hand, are linked to the coalescence of binary compact objects (NS-NS or BH-NS)[1] that result in kilonovae[2] (KNe) [sGRBs; $T_{90} \lesssim 2$ s; 6–10].

It is thought that enormous volumes of materials with a wide range of velocities are propelled in both cases. Non-relativistic ejecta masses such as dynamical ejecta, cocoon material, shock breakout material, and wind ejecta are propelled in NS-NS mergers [e.g., see 11–14] with velocities in the range $0.03 \lesssim \beta \lesssim 0.8$ (expressed, hereafter, in units of the speed of light). Similarly, several ejecta masses with non-relativistic velocities smaller than $\beta \lesssim 0.3$ have also been observed in the context of CC-SNe.

The interaction of the ejecta mass with the surrounding circumburst medium was suggested to characterize multi-wavelength afterglow observations on time scales ranging from days to many years in the non-relativistic domain [e.g., see 15–21]. Several authors, [e.g see 22–26], took into account the material launched during the coalescence of binary compact objects and computed the synchrotron emission in the radio bands. The authors assumed the existence of a free-coasting phase before the Sedov-Taylor expansion. Tan et al. [27] hypothesized that the shock wave's kinetic energy may be characterized by a power-law (PL) velocity distribution. Ever since, several authors have proposed that the material ejected during binary compact object coalescence and the CC-SNe be characterized by a PL velocity distribution [e.g., see 10, 13, 28–39].

In this proceedings, we provide a theoretical model that predicts the late-time multi-wavelength afterglow emission created by the deceleration of the outermost non-relativistic ejecta mass in a circumstellar medium. We assume interaction with a medium parametrized by a power law density profile $n(r) \propto r^{-k}$. We also express the equivalent kinetic energy of the outermost matter as a power-law velocity distribution $E \propto (\Gamma\beta)^{-\alpha}$. Finally, we consider a long-lasting central engine with the kinetic energy as a power-law distribution $E \propto t^{1-q}$.

The ejecta mass begins to decelerate after a long time, when the swept up quantity of material is similar to the ejected mass. Electrons are accelerated in forward shocks and cooled down by synchrotron radiation during this stage. We present the predicted synchrotron light curves for k = 0, 1, 1.5, 2 and 2.5 that cover several ejecta masses launched during the coalescence of binary compact objects and the CC-SNe.

The paper is organized as follows: In Section 2, we introduce the theoretical model that predicts the multi-wavelength afterglow emission generated by the deceleration of the non-relativistic ejecta mass.

We assume for the cosmological constants a spatially flat universe ΛCDM model with $H_0 = 69.6\,\mathrm{km\,s^{-1}\,Mpc^{-1}}$, $\Omega_\mathrm{M} = 0.286$ and $\Omega_\Lambda = 0.714$ [40]. Prime and unprimed quantities are used for the comoving and observer frames, respectively.

[1] NS corresponds to neutron star and BH to black hole.

[2] A fairly isotropic thermal transient powered by the radioactive decay of rapid neutron capture process nuclei and isotopes

2. Theoretical Model

We model the afterglow as two components. The first one is the nonrelativistic ejecta mass ($\Gamma \approx 1$). The second one is as the first one with the addition of the energy injection model:

$$E_2(t) = \tilde{E}_{\rm inj} t^{1-q}. \tag{1}$$

The first component is assumed to follow a spherical profile of the form [41]

$$E_1 = \tilde{E}\,(\Gamma\beta)^{-\alpha} \approx \tilde{E}\beta^{-\alpha}, \tag{2}$$

where β is the shock front's velocity and $\Gamma \sim 1$ its Lorentz factor. In the nonrelativistic regime, the ejecta mass is described by the Sedov–Taylor solution. Then, the velocity can be written as

$$\beta = \beta^0\ (1+z)^{\frac{3-k}{5-k}}\ A_{\rm k}^{-\frac{1}{5-k}}\ E_T^{\frac{1}{5-k}}\ t^{\frac{k-3}{5-k}}\,, \tag{3}$$

where $E_T = E_1 + E_2$ with E_1 and E_2 are given in Eqs. (1) and (2) and where the density parameter is denoted by A_k and the redshift as z. Therefore, the Sedov–Taylor solution can be written in a general form as

$$\tilde{E}\beta^{-\alpha} + \tilde{E}_{\rm inj} t^{1-q} = \beta^{0^{k-5}}\,(1+z)^{k-3}\ A_{\rm k}\,\beta^{5-k}\,t^{3-k}\,. \tag{4}$$

With this in mind, we have two limiting cases:

$$\begin{cases} \tilde{E}\beta^{-\alpha} \propto (1+z)^{k-3}\ A_{\rm k}\,\beta^{5-k}\,t^{3-k}, & \tilde{E} >> \tilde{E}_{\rm inj}, \\ \tilde{E}_{\rm inj} t^{1-q} \propto (1+z)^{k-3}\ A_{\rm k}\,\beta^{5-k}\,t^{3-k}, & \tilde{E} << \tilde{E}_{\rm inj}. \end{cases} \tag{5}$$

Each limiting case leads to a different velocity; they are given by:

$$\begin{cases} \beta \propto (1+z)^{-\frac{k-3}{\alpha+5-k}}\ A_{\rm k}^{-\frac{1}{\alpha+5-k}}\ \tilde{E}^{\frac{1}{\alpha+5-k}}\ t^{\frac{k-3}{\alpha+5-k}}, & \tilde{E} >> \tilde{E}_{\rm inj}, \\ \beta \propto (1+z)^{\frac{k-3}{k-5}}\ A_{\rm k}^{\frac{1}{k-5}}\ \tilde{E}_{\rm inj}^{-\frac{1}{k-5}}\ t^{\frac{q+2-k}{k-5}}, & \tilde{E} << \tilde{E}_{\rm inj}. \end{cases} \tag{6}$$

Both cases may be written with just one expression:

$$\beta = \beta^0\ (1+z)^{-\frac{k-3}{\alpha+5-k}}\ A_{\rm k}^{-\frac{1}{\alpha+5-k}}\ \tilde{E}^{\frac{1}{\alpha+5-k}}\ t^{\frac{k-(q+2)}{\alpha+5-k}}\,, \tag{7}$$

where the case $\tilde{E} >> \tilde{E}_{\rm inj}$ is obtained by setting $q = 1$, while the case $\tilde{E} << \tilde{E}_{\rm inj}$ is obtained by setting $\alpha = 0$ and $\tilde{E} = \tilde{E}_{\rm inj}$. With this, we may also write the blast wave radius $r \propto (1+z)^{-1}\,\beta t$ as:

$$r = r^0\ (1+z)^{-\frac{\alpha+2}{\alpha+5-k}}\ A_{\rm k}^{-\frac{1}{\alpha+5-k}}\ \tilde{E}^{\frac{1}{\alpha+5-k}}\ t^{\frac{\alpha+3-q}{\alpha+5-k}}\,. \tag{8}$$

Synchrotron emission We assume an electron distribution described as $dN/d\gamma_e \propto \gamma_e^{-p}$ for $\gamma_e \geq \gamma_m$, where p is the index of the elctron distribution and γ_m is the Lorentz factor of the lowest-energy electrons. During the deceleration phase, the electron Lorentz factors and the post-shock magnetic field evolve as, $\gamma_{\rm m} \propto t^{\frac{2(k-(q+2))}{\alpha+5-k}}$, $\gamma_{\rm c} \propto t^{\frac{-1+2q-k(-2+q-\alpha)-\alpha}{\alpha+5-k}}$, and $B' \propto t^{-\frac{-4-k-2q+kq-k\alpha}{2(\alpha+5-k)}}$, respectively. The corresponding synchrotron break frequencies and max flux density are given by:

$$
\begin{aligned}
\nu_{\rm m}^{\rm syn} &\propto (1+z)^{\frac{20+k(\alpha-6)-2\alpha}{2(\alpha+5-k)}}\ \epsilon_{\rm e}^{2}\,\epsilon_{\rm B}^{\frac{1}{2}}\,A_{\rm k}^{\frac{\alpha-5}{2(\alpha+5-k)}}\,\tilde{E}^{\frac{10-k}{2(\alpha+5-k)}}\,t^{-\frac{10(2+q)+k(-7-q+\alpha)}{2(\alpha+5-k)}}\\
\nu_{\rm c}^{\rm syn} &\propto (1+z)^{-\frac{8-2\alpha+k(3\alpha+2)}{2(\alpha+5-k)}}\ \epsilon_{\rm B}^{-\frac{3}{2}}\,(1+Y)^{-2}\,A_{\rm k}^{-\frac{3(\alpha+3)}{2(\alpha+5-k)}}\,\tilde{E}^{\frac{3(k-2)}{2(\alpha+5-k)}}\,t^{-\frac{8-6q+k(-7+3q-3\alpha)+4\alpha}{2(\alpha+5-k)}}\\
F_{\nu,\rm max}^{\rm syn} &\propto (1+z)^{\frac{4+2k-4\alpha+3k\alpha}{2(\alpha+5-k)}}\ \epsilon_{\rm B}^{\frac{1}{2}}\,D_{\rm z}^{-2}\,A_{\rm k}^{\frac{3\alpha+7}{2(\alpha+5-k)}}\,\tilde{E}^{\frac{8-3k}{2(\alpha+5-k)}}\,t^{\frac{14-8q+k(-7+3q-3\alpha)+6\alpha}{2(\alpha+5-k)}},
\end{aligned}
\tag{9}
$$

where Y is the Compton parameter, D_z is the luminosity distance, ϵ_e is the fraction of the shock's thermal energy density that is transmitted to the electrons and ϵ_B is the fraction turned into magnetic energy density [20].

Using the synchrotron break frequencies and the spectral peak flux density (eq. 9), the synchrotron light curves in the fast- and slow-cooling regime are:

$$
F_{\nu}^{\rm syn} \propto \begin{cases} t^{\frac{25-15q+2k(-7+3q-3\alpha)+11\alpha}{3(\alpha+5-k)}}\,\nu^{\frac{1}{3}}, & \nu < \nu_{\rm c}^{\rm syn},\\ t^{\frac{20-10q+k(-7+3q-3\alpha)+8\alpha}{4(\alpha+5-k)}}\,\nu^{-\frac{1}{2}}, & \nu_{\rm c}^{\rm syn} < \nu < \nu_{\rm m}^{\rm syn},\\ t^{-\frac{10p(2+q)-8(5+\alpha)+kp(-7-q+\alpha)+2k(7-q+\alpha)}{4(\alpha+5-k)}}\,\nu^{-\frac{p}{2}}, & \nu_{\rm m}^{\rm syn} < \nu, \end{cases}
\tag{10}
$$

and

$$
F_{\nu}^{\rm syn} \propto \begin{cases} t^{\frac{31-7q+2k(-7+2q-2\alpha)+9\alpha}{3(\alpha+5-k)}}\,\nu^{\frac{1}{3}}, & \nu < \nu_{\rm m}^{\rm syn},\\ t^{-\frac{10p(2+q)+6(-8+q-2\alpha)+k(21-5q+5\alpha+p(-7-q+\alpha))}{4(\alpha+5-k)}}\,\nu^{-\frac{p-1}{2}}, & \nu_{\rm m}^{\rm syn} < \nu < \nu_{\rm c}^{\rm syn},\\ t^{-\frac{10p(2+q)-8(5+\alpha)+kp(-7-q+\alpha)+2k(7-q+\alpha)}{4(\alpha+5-k)}}\,\nu^{-\frac{p}{2}}, & \nu_{\rm c}^{\rm syn} < \nu, \end{cases}
\tag{11}
$$

respectively.

3. Results and discussion

Figure 1 shows examples of synchrotron light curves with this model. The purple curves stand for X-ray (1 keV), the green ones for optical (1 eV) and the blue ones for radio (1.6 GHz). Panels 1a and 1b correspond to a model without energy injection in an ISM and wind-like medium, respectively. Panel 1c shows the curves in a wind-like medium for the energy injection component. In all cases, an increase of the stratification parameter leads to a flattening of the rising flux and a steepening of the decreasing one. In the case of radio band, it also leads to the appearance of a double peak. By comparing the first two panels with the third one, it can be seen that the energy injection model leads to larger fluxes by about two orders of magnitude. The right panel also shows that the decrease of the flux starts at much later times than in models without energy injection.

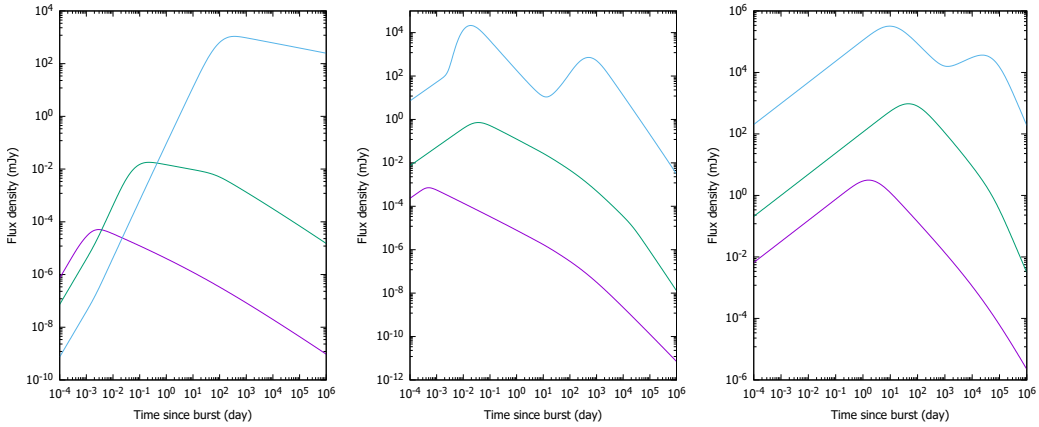

(a) ISM $k = 0$. **(b)** Wind $k = 2$ **(c)** Wind $k = 2$ and $q = 0.8$.

Figure 1: Synchrotron light curves from a sub-relativistic material decelerated in different circumburst media.

The parameters used for Figure 1a are: $\tilde{E} = 10^{51}$ erg, $\epsilon_B = 10^{-2}$, $\epsilon_e = 10^{-1}$, $A_k = 1$ cm^{-3}, $p = 2.8$, $q = 1.0$, $\alpha = 3.0$, $D_z = 100$ Mpc and $z = 0.022$.

For Figure 1b, they are: $\tilde{E} = 10^{51}$ erg, $\epsilon_B = 10^{-2}$, $\epsilon_e = 10^{-1}$, $A_k = 3 \times 10^{36}$ cm^{-1}, $p = 2.8$, $q = 1.0$, $\alpha = 3.0$, $D_z = 100$ Mpc and $z = 0.022$.

Finally, for Figure 1c, they are: $\tilde{E} = 10^{51}$ erg, $\epsilon_B = 10^{-2}$, $\epsilon_e = 10^{-1}$, $A_k = 3 \times 10^{36}$ cm^{-1}, $p = 2.6$, $q = 0.8$, $\alpha = 0$, $D_z = 100$ Mpc and $z = 0.022$.

4. Conclusion

We have derived a model that describes the non-relativistic, adiabatic evolution of the forward shock described by the Sedov-Taylor solution. We have modeled the afterglow in two components: one that considers a long-lasting central engine that injects energy into the shock, which leads to the power-law dependence $E \propto \tilde{E} t^{1-q}$; and one that doesn't assume energy injection and instead assumes a power-law energy distribution $E \propto (\Gamma\beta)^{-\alpha}$. We have also taken into account that the ejecta interacts with a medium parametrized by a power law number density distribution $A \propto R^{-k}$. This general approach is advantageous, as it allows one to not only consider a homogeneous medium ($k = 0$) and a wind-like medium ($k = 2$), but regions with non-standard stratification parameters, in particular $k = 1$, 1.5 or 2.5. It also allows one to transition between energy injection models to models without it by the change of two parameters: α and β.

We have calculated, for both components, the synchrotron light curves in the fast- and slow-cooling regimes and we have analyzed their behaviour for different sets of parameters. In the case of variation of the stratification parameter, we have noticed that an increase of this parameter leads to flatter profiles when the flux increases. It also leads to the appearance of a double-peak behavior in the radio band. As for the case of the comparison between energy injection with models without it, we have shown that the flux increases in general and the moment when it begins to decrease happens later when energy injection is considered.

Acknowledgments

We acknowledge the support from Consejo Nacional de Ciencia y Tecnología (CONACyT), México, grants IN106521

References

[1] C. Kouveliotou, C.A. Meegan, G.J. Fishman, N.P. Bhat, M.S. Briggs, T.M. Koshut et al., *Identification of Two Classes of Gamma-Ray Bursts*, **413** (1993) L101.

[2] J.S. Bloom, S.R. Kulkarni, S.G. Djorgovski, A.C. Eichelberger, P. Côté and et al., *The unusual afterglow of the γ-ray burst of 26 March 1998 as evidence for a supernova connection*, **401** (1999) 453 [astro-ph/9905301].

[3] S.E. Woosley and J.S. Bloom, *The Supernova Gamma-Ray Burst Connection*, **44** (2006) 507 [astro-ph/0609142].

[4] S.E. Woosley, *Gamma-Ray Bursts from Stellar Mass Accretion Disks around Black Holes*, **405** (1993) 273.

[5] T.J. Galama, P.M. Vreeswijk, J. van Paradijs, C. Kouveliotou, T. Augusteijn, H. Böhnhardt et al., *An unusual supernova in the error box of the γ-ray burst of 25 April 1998*, **395** (1998) 670 [astro-ph/9806175].

[6] L.-X. Li and B. Paczyński, *Transient Events from Neutron Star Mergers*, **507** (1998) L59 [astro-ph/9807272].

[7] S. Rosswog, *Mergers of Neutron Star-Black Hole Binaries with Small Mass Ratios: Nucleosynthesis, Gamma-Ray Bursts, and Electromagnetic Transients*, **634** (2005) 1202 [astro-ph/0508138].

[8] B.D. Metzger, G. Martínez-Pinedo, S. Darbha, E. Quataert, A. Arcones, D. Kasen et al., *Electromagnetic counterparts of compact object mergers powered by the radioactive decay of r-process nuclei*, **406** (2010) 2650 [1001.5029].

[9] D. Kasen, N.R. Badnell and J. Barnes, *Opacities and Spectra of the r-process Ejecta from Neutron Star Mergers*, **774** (2013) 25 [1303.5788].

[10] B.D. Metzger, *Kilonovae*, *Living Reviews in Relativity* **20** (2017) 3 [1610.09381].

[11] S. Goriely, A. Bauswein and H.-T. Janka, *r-process Nucleosynthesis in Dynamically Ejected Matter of Neutron Star Mergers*, **738** (2011) L32 [1107.0899].

[12] K. Hotokezaka, K. Kyutoku, M. Tanaka, K. Kiuchi, Y. Sekiguchi, M. Shibata et al., *Progenitor Models of the Electromagnetic Transient Associated with the Short Gamma Ray Burst 130603B*, **778** (2013) L16 [1310.1623].

[13] A. Bauswein, S. Goriely and H.T. Janka, *Systematics of Dynamical Mass Ejection, Nucleosynthesis, and Radioactively Powered Electromagnetic Signals from Neutron-star Mergers*, **773** (2013) 78 [1302.6530].

[14] S. Wanajo, Y. Sekiguchi, N. Nishimura, K. Kiuchi, K. Kyutoku and M. Shibata, *Production of All the r-process Nuclides in the Dynamical Ejecta of Neutron Star Mergers*, **789** (2014) L39 [1402.7317].

[15] R.A.M.J. Wijers, M.J. Rees and P. Meszaros, *Shocked by GRB 970228: the afterglow of a cosmological fireball*, **288** (1997) L51 [astro-ph/9704153].

[16] Z.G. Dai and T. Lu, *The Afterglow of GRB 990123 and a Dense Medium*, **519** (1999) L155 [astro-ph/9904025].

[17] Y.F. Huang, Z.G. Dai and T. Lu, *A generic dynamical model of gamma-ray burst remnants*, **309** (1999) 513 [astro-ph/9906370].

[18] M. Livio and E. Waxman, *Toward a Model for the Progenitors of Gamma-Ray Bursts*, **538** (2000) 187 [astro-ph/9911160].

[19] Y.F. Huang and K.S. Cheng, *Gamma-ray bursts: optical afterglows in the deep Newtonian phase*, **341** (2003) 263 [astro-ph/0301387].

[20] L. Sironi and D. Giannios, *A Late-time Flattening of Light Curves in Gamma-Ray Burst Afterglows*, **778** (2013) 107 [1307.3250].

[21] R. Barniol Duran and D. Giannios, *Radio rebrightening of the GRB afterglow by the accompanying supernova*, **454** (2015) 1711 [1504.06322].

[22] B.D. Metzger and G.C. Bower, *Constraints on long-lived remnants of neutron star binary mergers from late-time radio observations of short duration gamma-ray bursts*, **437** (2014) 1821 [1310.4506].

[23] W. Fong, B.D. Metzger, E. Berger and F. Özel, *Radio Constraints on Long-lived Magnetar Remnants in Short Gamma-Ray Bursts*, **831** (2016) 141 [1607.00416].

[24] L.-D. Liu, H. Gao and B. Zhang, *Constraining the Long-lived Magnetar Remnants in Short Gamma-Ray Bursts from Late-time Radio Observations*, **890** (2020) 102 [1912.00399].

[25] G. Schroeder, B. Margalit, W.-f. Fong, B.D. Metzger, P.K.G. Williams, K. Paterson et al., *A Late-time Radio Survey of Short GRBs at $z < 0.5$: New Constraints on the Remnants of Neutron Star Mergers*, *arXiv e-prints* (2020) arXiv:2006.07434 [2006.07434].

[26] N. Fraija, F. De Colle, P. Veres, S. Dichiara, R. Barniol Duran, A. Galvan-Gamez et al., *The Short GRB 170817A: Modeling the Off-axis Emission and Implications on the Ejecta Magnetization*, **871** (2019) 123.

[27] J.C. Tan, C.D. Matzner and C.F. McKee, *Trans-Relativistic Blast Waves in Supernovae as Gamma-Ray Burst Progenitors*, **551** (2001) 946 [astro-ph/0012003].

[28] K. Kyutoku, K. Ioka and M. Shibata, *Ultrarelativistic electromagnetic counterpart to binary neutron star mergers*, **437** (2014) L6 [1209.5747].

[29] K. Hotokezaka and T. Piran, *Mass ejection from neutron star mergers: different components and expected radio signals*, **450** (2015) 1430 [1501.01986].

[30] R. Barniol Duran, E. Nakar, T. Piran and R. Sari, *The afterglow of a relativistic shock breakout and low-luminosity GRBs*, **448** (2015) 417 [1407.4475].

[31] K.P. Mooley, E. Nakar, K. Hotokezaka, G. Hallinan, A. Corsi, D.A. Frail et al., *A mildly relativistic wide-angle outflow in the neutron-star merger event GW170817*, **554** (2018) 207 [1711.11573].

[32] N. Fraija, A.C.C.d.E.S. Pedreira and P. Veres, *Light Curves of a Shock-breakout Material and a Relativistic Off-axis Jet from a Binary Neutron Star System*, **871** (2019) 200.

[33] A. Kathirgamaraju, D. Giannios and P. Beniamini, *Observable features of GW170817 kilonova afterglow*, **487** (2019) 3914 [1901.00868].

[34] B.D. Metzger, *Kilonovae*, *Living Reviews in Relativity* **23** (2019) 1 [1910.01617].

[35] D. Lazzati, B.J. Morsony, C.H. Blackwell and M.C. Begelman, *Unifying the Zoo of Jet-driven Stellar Explosions*, **750** (2012) 68 [1111.0970].

[36] A. Horesh, S.R. Kulkarni, A. Corsi, D.A. Frail, S.B. Cenko, S. Ben-Ami et al., *PTF 12gzk—A Rapidly Declining, High-velocity Type Ic Radio Supernova*, **778** (2013) 63 [1306.5755].

[37] R. Margutti, A.M. Soderberg, M.H. Wieringa, P.G. Edwards, R.A. Chevalier and et al., *The Signature of the Central Engine in the Weakest Relativistic Explosions: GRB 100316D*, **778** (2013) 18 [1308.1687].

[38] R. Margutti, D. Milisavljevic, A.M. Soderberg, C. Guidorzi, B.J. Morsony, N. Sanders et al., *Relativistic Supernovae have Shorter-lived Central Engines or More Extended Progenitors: The Case of SN 2012ap*, **797** (2014) 107 [1402.6344].

[39] N. Fraija, F. De Colle, P. Veres, S. Dichiara, R. Barniol Duran, A.C. Caligula do E. S. Pedreira et al., *Description of Atypical Bursts Seen Slightly Off-axis*, **896** (2020) 25 [1906.00502].

[40] Planck Collaboration, P.A.R. Ade, N. Aghanim, M. Arnaud, M. Ashdown, J. Aumont et al., *Planck 2015 results. XIII. Cosmological parameters*, **594** (2016) A13 [1502.01589].

[41] N. Fraija, B.B. Kamenetskaia, M.G. Dainotti, R.B. Duran, A. Gálvan Gámez, S. Dichiara et al., *Afterglow Light Curves of Nonrelativistic Ejecta Mass in a Stratified Circumstellar Medium*, **907** (2021) 78 [2006.04049].